Influences of Operational Parameters on Methylene Blue Degradation in the Suspension Photoreactor Using Aeroxide® P25/TiO₂ as a Photocatalyst

Khatcharin Wetchakun[1,*], Natda Wetchakun[2,3]

[1]*Faculty of Science, Ubon Ratchathani Rajabhat University, Ubon Ratchathani, 34000, Thailand*
[2]*Photocatalysts and 2D Materials Research Laboratory, Department of Physics and Materials Science, Faculty of Science, Chiang Mai University, Chiang Mai, 50200, Thailand*
[3]*Center of Excellence in Materials Science and Technology, Chiang Mai University, Chiang Mai, 50200, Thailand*

ABSTRACT

Degradation of methylene blue (MB) by photocatalytic process and utilization of Aeroxide® P25 as a photocatalyst for purifying water have been abundantly researched. Evonik (formerly Degussa) Aeroxide® TiO₂ P25 (denoted as P25), produced by flame pyrolysis of TiCl₄ vapor, is a popular photocatalyst material for use as the photocatalyst reference due to its high photocatalytic efficiency. This research aims to investigate and discover the most effective operational parameters on the photocatalytic degradation of methylene blue using Aeroxide® P25 as a photocatalyst. In the experiment, the MB degradation kinetics of varying four operational parameters in heterogeneous photocatalytic system composed of the 50 mL suspension photoreactor, MB and Aeroxide® P25 were investigated by UV-Vis spectroscopy. The variable operational parameters consist of Aeroxide® P25 concentration, agitation speed, pH and light intensity. The fixed operational parameters consist of initial concentration of MB (11.6 ± 0.8 mg L^{-1}), air ambient and temperature (25 ± 1 ºC). The reductions of MB concentrations were fitted well with a pseudo-first order kinetic model, and then the apparent reaction rate constants (k_{app}) were reported. The correlation between the k_{app} values and amounts of the operational parameters was fitted to predict trends. Moreover, influence of irradiating light regions over the photocatalytic degradation was investigated. The dispersion stability of Aeroxide® P25 in water from varying pH of the suspension was also investigated for supporting the analysis of this work. The operational parameters were arranged in order of influence on MB degradation performance from using Aeroxide® P25 as a photocatalyst in the

suspension photoreactor as the result: UVA light intensity > Agitation speed $\cong$ pH > Concentration of Aeroxide® P25. The optimal condition for operating MB photocatalytic degradation using Aeroxide® P25 as a photocatalyst in our system is MB concentration of ~12 mg L^{-1}, Aeroxide® P25 concentration of 4-5 g L^{-1}, pH 9.2, light intensity of 412 μW cm^{-2} and agitation speed of 2500 rpm.

Keywords: Aeroxide® P25; Methylene blue degradation; Operational parameters; Photocatalysis; TiO_2

1. Introduction

Methylene blue (MB) is a cationic dye used in several fields including medicine, biology and chemistry. MB has been injected into parathyroid glands for facilitating in surgery. MB used as a safe drug for parathyroidectomy showed its dose of less than 2 mg/kg. Moreover, just as an MB dose reaches the range of 5–10 mg/kg, it probably affects the central nervous system (CNS) which might induce prolonged disorientation in the postoperative period [1] and potentially fatal serotonin toxicity [2]. Moreover, MB also affects Alzheimer's disease and cancer [3]. MB should be used at a dose not exceeding 4 mg/kg on the UK National Poisons Information Service recommendations [4]. MB is possible to be contaminated with water resources comprising groundwater and surface water. The adsorption, chemical coagulation and membrane filtration are possible processes for using in MB separation from water. Among these processes, MB is transferred to attach materials target, but it is not decomposed. To decompose MB in water, using photolysis under sunlight irradiation and non-basic condition may have not sufficient efficiency.

MB removal from water using a photocatalysis process has become an efficient technique for degrading toxic organic molecules including methylene blue (MB) in water, so several researches have focused on it. Moreover, the photocatalytic reactor type for degrading MB in water using mobilized photocatalyst excited by matchable light source, named suspension photoreactor or slurry photocatalytic reactor, have gained interest from many researchers due to the effective specific surface area of the photocatalysts. From previous researches, there is usage of various photocatalysts for degrading MB in water such as Fe^{3+}-doped TiO_2 [5], Cu-doped $SrTiO_3$ [6], Fe_3O_4-embedded graphene oxide [7], $NaInO_2$ [8], Hafnium-doped ZnO [9], $NiMoO_4$ [10], ZnS/CdS [11], Sr/CdSe [12], etc. However, many researches have focused on TiO_2 in commercial form named Aeroxide® P25 for purifying water with the photocatalytic process for the reason that Aeroxide® P25 has good photocatalytic efficiency due to its properties such as high surface area, weak visible light harvesting ability, and low recombination between electrons and holes from having its composition of anatase and rutile phases [13, 14].

Aeroxide® TiO_2 P25 is a fine-particulate pure titanium dioxide (TiO_2) with high specific surface, and has marked aggregate and agglomerate structure. Because of its high purity, high specific surface area and unique combination of anatase and rutile crystal structure, the product is suitable for many catalytic and photocatalytic applications. Its structure also makes it suitable for use as an effective UV filter. Moreover, electric charges in mixed-phase TiO_2 can be produced under visible light via rutile phase and then transferred to anatase phase which have lower energy [15]. Phase composition of Aeroxide® P25 from Aldrich was analyzed by X. Jiang et al. [16], and the result was that it is composed of anatase (77.1%), rutile (15.9%) and amorphous TiO_2 (7.0%). The presented the

possible microstructures of Aeroxide® P25 as consisting of mainly individual anatase and rutile nanoparticles and a heterojunction structure of a thin rutile overlayer on anatase surface from Moiré fringes by TEM analysis, and showed that the primary particle sizes, surface area and pore size of Aeroxide® P25 were 10-50 nm, 60. 8 m^2/g and 17.8 nm, respectively. In 2001, A. Houas et al. [17] investigated the photocatalytic degradation pathway of methylene blue in water using titania Degussa P-25 as a photocatalyst under UV irradiation. The particular aromatics as intermediate products identified under the degradation pathway consist of successive hydroxylations leading to the aromatic ring opening. The final products of the almost complete mineralization of MB were CO_2, NH_4^+, NO_3^- and SO_4^{2-}.

In earlier studies, experimental data of various operational parameters affecting photocatalytic degradations of toxic organic compounds, including many toxic dyes, were analyzed and optimized through the kinetic-based models. The models provided the correlation between apparent reaction rate constant or initial rate of the photocatalytic degradation of the dyes and amount of those parameters. For example, a dynamic model of photocatalytic degradation of para-nitrophenol (PNP) using TiO_2 nanofiber as a photocatalyst by varying two operational parameters consisting of light intensity and photocatalyst loading was reported by N. Singh et al. [18]. They gave the explanation that the degradation rate of the organic molecules directly depended on the reaction rate. The kinetic model description and optimization of photocatalytic removal of rhodamine 6G (Rh-6G) using polyaniline/ZnS nanocomposite as a photocatalyst were reported by S. Allahveran and A. Mehrizad [19] through varying initial concentration of dye, concentration of

photocatalyst, pH and light intensity. They reported that the most important variable for removing Rh-6G was irradiation time. M. Ebrahimi et al. [20] created a photo-degradetion kinetic model via the experiment of photocatalytic degradation of MB and methyl orange (MO) using ZnO nanowire as a photocatalyst. They found that the correlation between photodegradation rate constant and branch length of ZnO nanowires revealed a linear function.
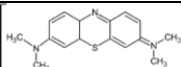
To the best of our knowledge, there have been no reports of analysis and evaluation of the most important operational parameters on photocatalytic degradation of MB using mobilized Aeroxide® P25 as a photocatalyst in the suspension photoreactor. This research aims to do this via the experimental investigation of MB degradation kinetics in the suspension photoreactor under variations of Aeroxide® P25 concentration, agitation speed, pH and light intensity using the UV-Vis spectroscopy technique. In addition, this research also aims to investigate dispersion stability of Aeroxide® P25 in water from varying pH values of the suspension for supporting the evaluation. The effect of photolysis was also carried out under the investigation of influence of light ranges over photocatalytic degradation of MB.

2. Materials and Methods
2.1 Materials

Methylene blue ($C_{16}H_{18}N_3ClS$) was dissolved in deionized water (RCI Labscan, Thailand) for testing the photodegradation with the prototype photocatalytic reactor. The structure and characteristic of methylene blue compound highlighted above are illustrated in Table 1.

Table 1. Structure and characteristic of methylene blue [21].

Type of dye	Example	Color index	λ_{max} (nm)	Structure
Cationic heterocyclic dye	Methylene Blue	C.I. 52015	665	

Titanium (IV) oxide, Aeroxide® P25 (Aldrich, Germany; ≥ 99.5% trace metals basis; particles size: 21 nm (TEM); surface area: 35-65 m^2 g^{-1}; molecular weight: 79.87 g/mol; CAS-No.: 13463-67-7) was used as a photocatalyst for testing photocatalytic degradation of MB. Perchloric acid 70% (QRec, New Zealand) and sodium hydroxide 99% (RCI-Labscan, Thailand) in analytical grade were used for adjusting pH values.

2.2 Dispersion stability tests of Aeroxide® P25 in water

The suspension of 4 g L^{-1} Aeroxide® P25 nanoparticles in deionized water was ultrasonicated for 10 min. The suspension was adjusted to pH values in the range of 2.1-11.1 with 0.02 M NaOH or $HClO_4$ under stirring, and then was continuously stirred for 30 min. The suspension was transferred to a borosilicate glass tube used as an optical cell with a diameter of 2.5 cm, and then it was placed in the cell box, having a rectangular-hole area of height × width: 2.0×1.0 cm, at the middle between the lamp and light detector with a constant distance of 15 cm. A 7 W LED bulb cool daylight lamp (E27), Philips, Netherlands, was used as a light source. A TM-208 visible light meter, Tenmars, Taiwan, was used as a light detector. The light intensities were continuously automatically detected using Light Meter TM-184 software, Tenmars.

2.3 Photocatalytic degradation tests of MB

MB solution was prepared in 50 ml with its initial concentration of 11.6 ± 0.8 mg L^{-1} for testing photocatalytic degradation of MB. The Aeroxide® P25 concentrations were varied in the range of 1-7 g L^{-1}. The suspension of Aeroxide® P25 nanoparticles was transferred to a borosilicate bottle (reaction bottle) having a bottom diameter of 5.6 cm and top diameter of 3.0 cm, and then its pH was adjusted to 2.7, 4.9 and 9.2 with 0.02 M NaOH or percholic acid. After that, the MB solution was transferred to the borosilicate bottle covered with a cap under ambient air, and then it was stirred under dark condition for 50 min. The suspension in the borosilicate bottle without a cap was tested under UVA light irradiation inside the prototype photocatalytic reactor with flat-plate collector under ambient air and a temperature of 25 ± 1 ºC. A 10 W blacklight fluorescent lamp (F01T8 BLB), Santory, Japan, was used as an UVA light source for exciting the photocatalyst. UVA intensities were varied in the range of 220-412 $\mu W/cm^2$, and the irradiation duration was in the range of 90-250 min. The MB samples were collected at that time, and then they were centrifuged twice at 13000 rpm with a microcentrifuge machine (ScanSpeed, Labogene, Denmark) for 5 min. The photolysis using UVA and visible light irradiations was performed to compare with the photocatalysis using UVA and visible light irradiations. Under visible light irradiation, a 10 W cool daylight fluorescent lamp (TL-D 10W/54-765), Philips, China, was used as a visible light source. Absorbance of the MB samples was measured by T90+ PG Instruments spectrophotometer. The UVA light intensity at the middle bottom surface of the borosilicate glass was measured by using TM-208 UVA light meter, Tenmars, Taiwan.

2.4 Photocatalytic analysis

The initial rate of the photocatalytic degradation (r_0) represented by $k_{app}C_0$ after UVA irradiation was analyzed from experimental data following a pseudo-first order kinetic model according to the Langmuir-Hinshelwood (L-H) kinetics model summarized as follows:

$$\ln\left(\frac{C_0}{C_t}\right) = -k_{app}t; \; k_{app} = \frac{kK}{1+KC_0}, \qquad (2.1)$$

$$r_0 = k_{app}C_0, \qquad (2.2)$$

where k_{app} is the apparent reaction rate constant, k is the reaction rate constant (mg L^{-1} min^{-1}), K is the adsorption constant (L mg^{-1}) and C_0 is the initial concentration (mg L^{-1}). The half time $(T_{1/2})$ of MB photocatalytic degradation, was given as the equation:

$$T_{1/2} = \frac{\ln 2}{k_{app}} \qquad (2.3)$$

The photodegradation efficiency $(\eta(\%))$ was calculated by the following equation:

$$\eta(\%) = \left(1 - \frac{C_t}{C_0}\right) \times 100 \qquad (2.4)$$

The kinetic models between k_{app} and amount of the operational parameters were also reported.

3. Results and Discussion
3.1 Dispersion stability of Aeroxide® P25 in water

Figs. 1A and B show the correlation between various pH values of Aeroxide® P25 suspension and transmittance at running time. The result revealed that Aeroxide® P25 particles falling as a function of running time under deionized

water at pH ~7 is faster than that at other pH values, indicating the lowest dispersion stability of Aeroxide® P25 for all running times. The sedimentation of Aeroxide® P25 particles under deionized water at pH ~7 is rather fast because pH ~7 is close to pH$_{pzc}$ of Aeroxide® P25 under deionized water (6.8 ± 0.2) [22]. In this condition, the particles agglomerate to larger particles by using water binder, showing low static electricity repellence and steric hindrance repulsion (Fig. 2).
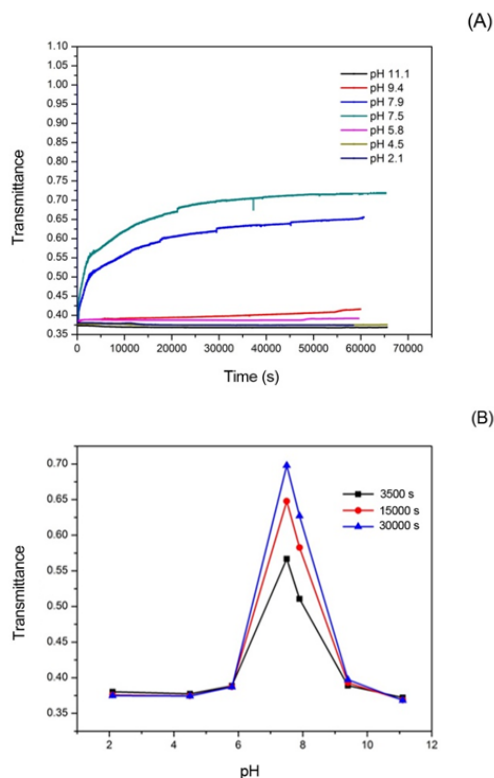

Fig. 1. (A) The correlation between transmittance and time (s) (B) the correlation between transmittance and pH of Aeroxide® P25 suspension under deionized water at running time of 3500, 15000 and 30000 s.
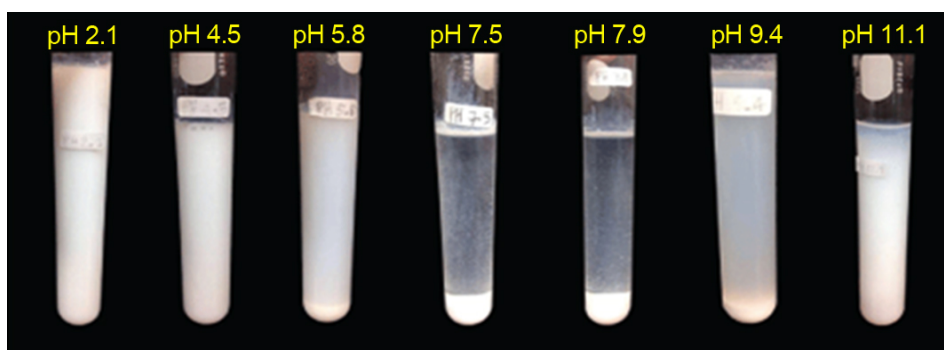
Fig. 2. Sedimentation of Aeroxide® P25 particles under deionized water at pH = 2.1, 4.5, 5.8, 7.9, 9.4 and 11.1 from left to right.

3.2 Photocatalytic degradation of MB

Two stages of apparent reaction rates appeared in the experimental results after UVA irradiation to the reaction bottle. The first stage of apparent reaction rates possibly results from instability of MB adsorption and desorption on the surface of the photocatalyst. The last stage of apparent reaction rates possibly results from the reaction of prominent hydroxyl radicals $\left(^{\bullet}OH\right)$ at the surface of the photocatalyst after the first stage [23]. The results were fitted into a pseudo-first order kinetic model in a single stage covering both stages since the first stage covered 30 min, and it has less influence on the fitted results. For example, Fig. 3 shows the effect of Aeroxide® P25 concentration variation on MB photocatalytic degradation. Moreover, each of the figures presented 3 patterns as follows: (A) the reduction in ratio of MB concentration at that time per initial MB concentration $\left(C_t / C_0\right)$ over UVA irradiation time (min), (B) pseudo-first order kinetic plots ($-\ln(C_t / C_0)$ vs. time (min)) of MB degradation under UVA irradiation and (C) the correlation between apparent reaction rate constant (k_{app}, min^{-1}) and number of operational parameters.

3.2.1 Influence of Aeroxide® P25 concentrations over photocatalytic degradation of MB

Fig. 4 shows that the variation of Aeroxide® P25 concentrations under the condition: MB concentration of ~12 mgL^{-1}, pH 4.9 (natural pH), light intensity of ~220 μW cm^{-2}, agitation speed of 1000 rpm and UVA irradiation, affect MB degradation. The k_{app} tendency of MB degradation increases at higher photocatalyst concentrations until a maximum photocatalyst concentration; after that, the k_{app} tendencies drop off because the higher turbidity reduces the penetration of light though water. They were fitted in an Exp3p2 exponential function (Fig. 4C):

$$k_{app} = \exp(a + bx + cx^2) \qquad (3.1)$$

The results showed that the optimal Aeroxide® P25 concentration used for the degradation of MB is 4-5 g L^{-1}.
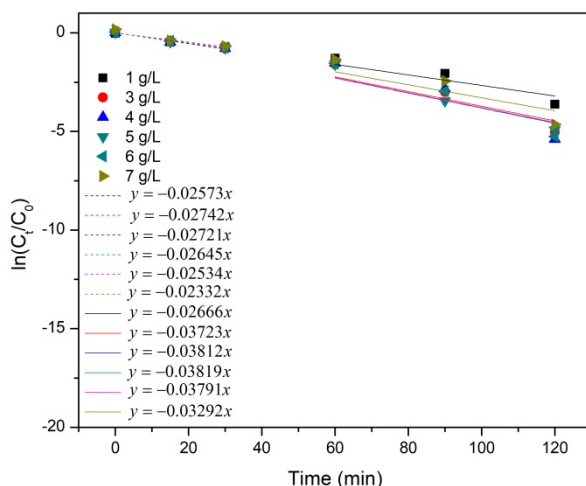
Fig. 3. Two stages of apparent reaction rates towards effect of Aeroxide® P25 concentration variation on MB photocatalytic degradation.
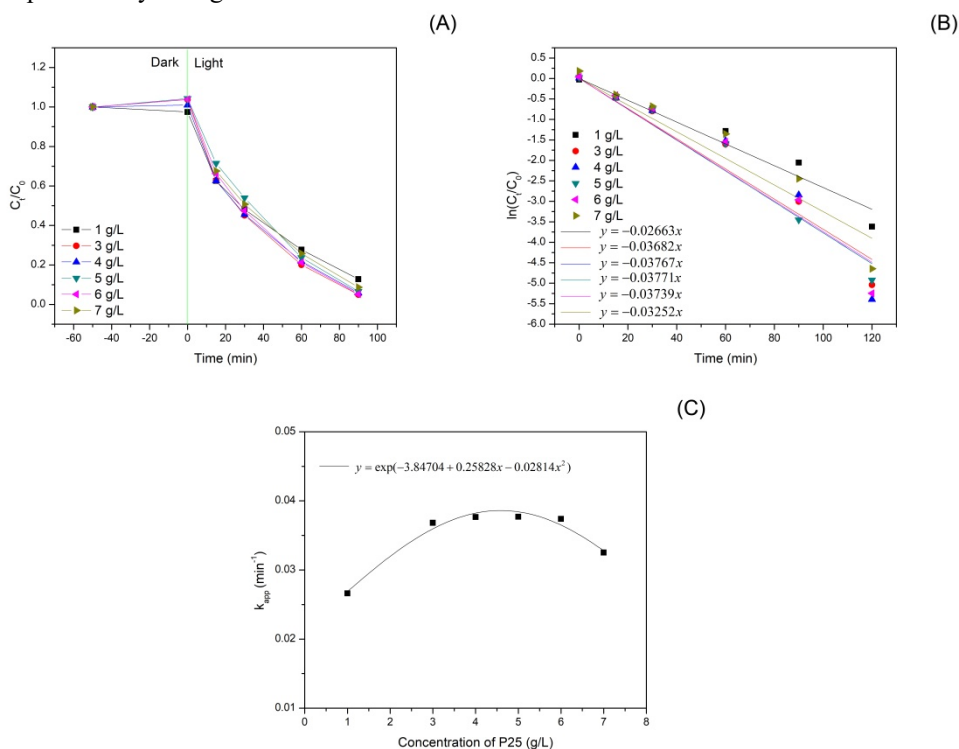

Fig. 4. Time-course variation of (A) C_t/C_0 and (B) $-\ln(C_t/C_0)$ and (C) k_{app} plot with different Aeroxide® P25 concentrations.

3.2.2 Influence of agitation speeds over photocatalytic degradation of MB

Fig. 5 shows that the variation of agitation speeds used in the photoreactor for degrading MB under the condition: MB concentration of ~12 mg L^{-1}, Aeroxide® P25 concentration of 4 g L^{-1}, pH 4.9 (natural pH) and light intensity of ~220 μW cm^{-2} and UVA irradiation, affects MB degradation. The k_{app} tendency of MB degradation to increase at higher agitation speeds was fitted in an allometric power function:

$$y = ax^b \qquad (3.2)$$

These results are similar to previous researches such as C.-H. Wu et al. and X. Wang et al. They provided that the k_{app} or r_0 tendencies of HF6 coral pink [26] and MB [5] degradations using the photocatalysts of undoped TiO$_2$ and Fe^{3+}-doped TiO$_2$, respectively, were fitted well with a power function, and the tendency of MB degradation increases due to increase of external mass transfer process. This is can be described by external transport effects on rates on solid-catalyzed reactions [29]. In the case, Fick's Law shows $N_{Ax} = -D_{AB}\dfrac{dC_A}{dx}$ where N_{Ax} is the flux of reactant A (catalyst) through the stagnant boundary layer surrounding a catalyst particle, x is a boundary position, and B is the bulk fluid (MB solution), and then the molar flux of A through the layer is $N_{Ax} = \dfrac{-D_{AB}}{\bar{\delta}}\left(C_{A\bar{\delta}} - C_{AS}\right)$ where $\bar{\delta}$ is thickness of the boundary layer, $C_{A\bar{\delta}}$ is the concentration of A at $x =$ the bulk fluid surface position, and C_{AS} is the concentration of A at $x =$ the catalyst surface position. The mass transfer coefficient is normally used since the magnitude of $\bar{\delta}$ is unknown. That is the average molar flux from the bulk fluid to the catalyst surface is $N_A = \bar{k}_c(C_{A\bar{\delta}} - C_{AS})$ where $\bar{k}_c$ is the mass transfer coefficient over the surface area of the catalyst particle. It correlates to the fluid velocity past the catalyst particle. If the fluid is well mixed, $C_{A\bar{\delta}}$ equals C_{AB}. Therefore, the equation can be written as: $N_A = \bar{k}_c\left(C_{AB} - C_{AS}\right)$. For a first-order reaction, the kinetics depend on the surface rate constant (k_s) and C_{AS}, and at steady-state, N_A equals the rate of reaction (r). Thus, the equation can be written as: $r = k_S C_{AS} = \bar{k}_c\left(C_{AB} - C_{AS}\right)$. It means that if $\bar{k}_c$ increases, the rate of reaction increases.

3.2.3 Influence of pH values over photocatalytic degradation of MB

The pH value in photocatalytic suspension affects the appearance of charges at the surface of photocatalysts causing ionic dyes probably attracted to surface of the photocatalysts. When the pH value in the suspension reaches the pH$_{pzc}$ value of Aeroxide® P25 particles (6.8 ± 0.2) under deionized water, these particles tend to aggregate to form larger particles. If the pH value of Aeroxide® P25 suspension is lower than its pH$_{pzc}$ value, the surface state of the photocatalyst is positive, and if the pH value of Aeroxide® P25 suspension is higher than its pH$_{pzc}$ value, the surface state of the photocatalyst is negative. MB is a tiazine dye with a chromophore attached to the positively charged sulphonic group and also known as basic dye. Therefore, in the case of MB, if the photocatalyst suspension exists under pH > pH$_{pzc}$ of the photocatalyst in water, MB carrying positive charges will be attached onto the negative surface of the photocatalyst. The adsorption process in the L-H model affects the efficiency of MB degradation via the

photocatalytic process. If the adsorption rate increases in the reaction, the efficiency of MB degradation also increases. In the photocatalytic process, the molecules of MB diffuse to active sites on the surface of Aeroxide® P25. This further provides reduction/ oxidation processes of photocatalytic degradation of MB.
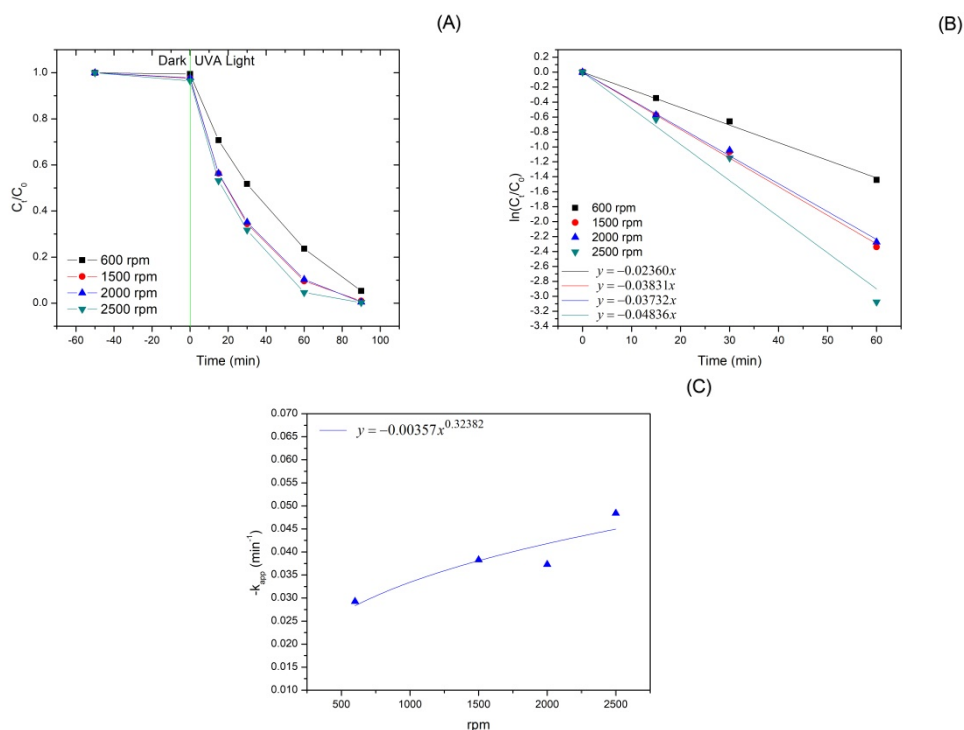

Fig. 5. Time-course variation of (A) C_t / C_0 and (B) $-\ln(C_t / C_0)$ and (C) k_{app} plot with different agitation speeds.

Fig. 6 shows that the variation of pH values adjusted in the suspension of MB and Aeroxide® P25 particles in deionized water for degrading MB under the condition: MB concentration of ~12 mgL^{-1}, light intensity of ~220 µW cm^{-2}, Aeroxide® P25 concentration of 4 g L^{-1}, agitation speeds of 0 and 600 rpm and UVA irradiation, affects MB degradation. The correlation between k_{app} and pH values is shown when the equation in fitted in an Exp3p2 exponential function as Eq. (3.1) (Figs. 5E and F). In the acidic region, at pH 2.7 and pH 4.9 (natural pH), the k_{app} values are low. On the other hand, at pH 9.2, the k_{app} value tends to steeply increase compared with the k_{app} values at pH 2.7 and pH 4.9. This is supported by the fact that pH 9.2 is more than the pH$_{pzc}$ value of Aeroxide® P25 in water. This is due to the adsorption process through electrostatic charges setting on both surfaces of MB and Aeroxide® P25 and high dispersion stability of Aeroxide® P25 in water. In Figs. 5A and 5B, MB adsorptions on Aeroxide® P25 surface can be clearly seen from the reduction of MB concentrations under dark conditions. pH values could be arranged in order of amount of MB adsorption on Aeroxide® P25 surface as the result: pH 9.2 > pH 2.7 > pH 4.9. The condition at pH 4.9 showed the lowest adsorption because a higher agglomeration of Aeroxide® P25 particles affects the low

specific surface area of Aeroxide® P25 and k_{app} value.

Under comparison between 0 rpm (without stirring) and 600 rpm (with stirring) of agitation speeds in same operational condition, the similar trends of the k_{app} values were found in Figs. 5E and 5F from varying pH values. Moreover, the results indicate that the k_{app} values from adjusting pH to 9.2 at 0 and 600 rpm are higher than those from adjusting pH to 2.4 as 6.37 and 1.46 times, respectively; conversely, the k_{app} values from adjusting agitation speed to 600 rpm at pH 2.4 and 9.2 are higher than those from adjusting

agitation speed to 0 rpm as 5.27 and 1.21 times, respectively. These indicate that both former results from changing pH values were more than both latter results from changing agitation speeds. Likewise, the results from testing dispersion stability of Aeroxide® P25 in water (Figs. 1 and 2) showed that the dispersion stability at pH 4.9 is lower than that at pH 2.7, but in the case of the absence of external agitation speeds (at 0 rpm), the k_{app} value at pH 4.9 is higher than that at pH 2.7. Therefore, the adjustment to the pH parameter which has more impact than the agitation speed should be focused to MB photocatalytic degradation.
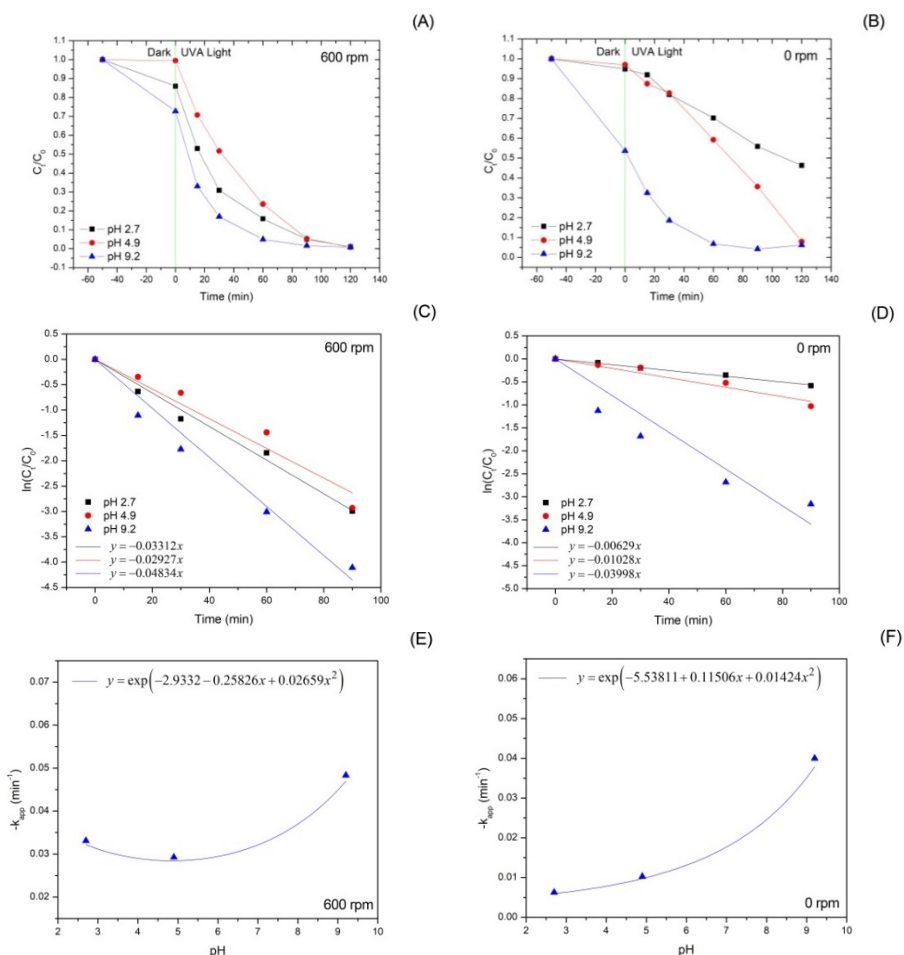

Fig. 6. Time-course variation of (A) C_t / C_0 and (B) $-\ln(C_t / C_0)$ and (C) k_{app} plot with different pH values.

3.2.4 Influence of light intensities over photocatalytic degradation of MB

Fig. 7 shows that the variation of the light intensities used in the photoreactor for degrading MB under the condition: MB concentration of ~12 mg L^{-1}, Aeroxide® P25 concentration of 4 g L^{-1}, pH 4.9 (natural pH) and agitation speed of ~1000 rpm and UVA irradiation, affects MB degradation. The k_{app} tendency of MB degradation increasing at higher UVA light intensities was fitted in a rational function:

$$y = (b + cx)/(1 + ax) \qquad (3.3)$$

Light intensity affects amounts of the excited electron-hole pairs in the photocatalyst which can assist in increasing the photocatalytic efficiency. On the other hand, electron-hole pairs generation depends on light energy or a light region which is more than or equal to the photocatalyst's band gap energy. Fig. 7 shows the relationship between UVA light intensities and the k_{app} values close to a linear function in the range of low UVA light intensities (220-323 μW cm^{-2}). These results are similar to previous research such as X. Wang et al. [5]. They provided that the k_{app} or r_0 tendency of dyes degradation fits well with a rational function. Moreover, N. Singh et al. [18] found that the k_{app} or r_0 tendency of dyes degradation fits well with a linear function in the range of low UVA light intensities.
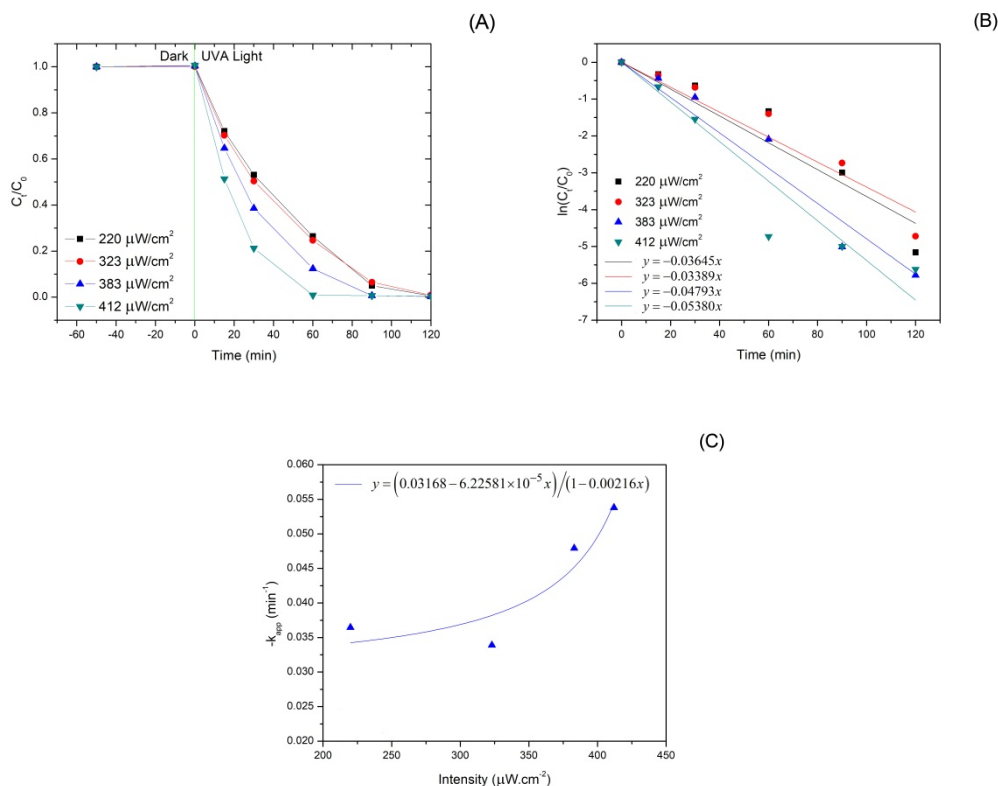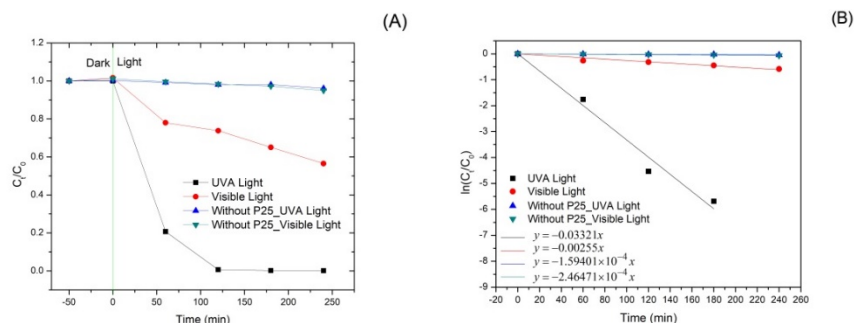
(A)

(B)

(C)

Fig. 7. Time-course variation of (A) C_t / C_0 and (B) $-\ln(C_t / C_0)$ and (C) k_{app} plot with different UVA light intensities.

3.2.5 Influence of light ranges over photocatalytic degradation of MB

Fig. 8 shows that the variation of the light ranges used in the photoreactor for degrading MB, under the condition: MB concentration of ~12 mg L^{-1}, Aeroxide® P25 concentration of 4 g L^{-1}, pH 4.9 (natural pH), light intensity of ~220 μW cm^{-2} and agitation speed of 1000 rpm, affects MB degradation. The deteriorations in percentage of MB concentrations without Aeroxide® P25 under UVA and visible light irradiations showed 4% and 6%, respectively. This indicates that MB is more sensitive to visible light than UVA light. Aeroxide® P25 can be sensitive under visible light irradiation because Aeroxide® P25 or Degussa P25 contains anatase: rutile in a ratio of approximately 3:1 [14]. Collapsing band energy states between anatase and rutile spreads photoactive range of rutile phase to visible light. This is a result of excited electrons from rutile transferring to anatase, affecting prevention of charge carriers' recombination [15].

Under visible light irradiation, the results show that the k_{app} value from the presence of Aeroxide® P25 as a photocatalyst is more than that from the absence of Aeroxide® P25 (Figs. 7A and 7B). However, its photocatalytic performance on MB degradation from the visible light irradiation is less than that from the UVA irradiation. The k_{app} value of the UVA light irradiation is more than that of the visible light irradiation by approximately 13 times, from the presence of Aeroxide® P25 as shown in Fig. 8C. To improve its visible light harvesting ability, its band gap can be adjusted by modifying its surface using alcohol solvothermal reduction [30] and using sulfanilic acid via hydrothermal treatment [31], including functionalizing with metals/non-metals/semiconductors [32-34]. These results are similar to previous research such as Y. Yang et al. [35]. They reported that the k_{app} value of MB degradation showed ~0.0076 min^{-1} using P25 as a photocatalyst under visible light irradiation from a 350 W xenon arc lamp having a cutoff filter (λ > 420 nm) under the conditions: room temperature, an initial MB concentration of 10 mg L^{-1}, and P25 concentration of 0.5 g L^{-1}. Therefore, the selection of light range matching with band gap of the photocatalyst in the first step is required for the photocatalytic degradation of toxic organic molecules.
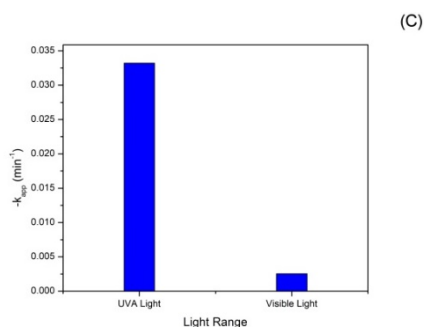
Fig. 8. Time-course variation of (A) C_t / C_0 and (B) $-\ln(C_t / C_0)$ and (C) k_{app} plot with different light ranges.

3.2.6 Summarization of the MB photocatalytic degradation on the k_{app}, $T_{1/2}$ and $\eta(\%)$ values affected by the operational parameters

Table 2 shows the trends of the operational parameters for MB photocatalytic degradation using Aeroxide® P25 powders as a photocatalyst fitted well with 3 functions as follows: (I) Exp3p2 exponential function, (II) allometric power function and (III) rational function. Aeroxide® P25 concentration and pH parameters provide an Exp3p2 exponential trend. The agitation speed parameter provides an allometric power trend. The UVA light intensity parameter provides a rational trend. Based on mathematical analysis, the highest increasing trend on the photodegradation of MB was found in the case of variation in Aeroxide® P25 concentrations from Eq. 3.4 in Table 2. However, the photocatalytic efficiency should be also considered through k_{app}, $T_{1/2}$ and $\eta(\%)$ analysis shown in Table 3. Table 3 shows the highest photocatalytic performance on the k_{app}, $T_{1/2}$ and $\eta(\%)$ values in each of the operational parameters. In Table 3, the operational parameters were ordered following the k_{app} value as follows: UVA light intensity > agitation speed $\cong$ pH > concentration of Aeroxide® P25. The

operational parameters were ordered following the $T_{1/2}$ value as follows: UVA light intensity < agitation speed $\cong$ pH < concentration of Aeroxide® P25. The operational parameters were ordered following the $\eta(\%)$ value as follows: UVA light intensity $\cong$ agitation speed > pH > concentration of Aeroxide® P25.

On the comparison of matching two conditions, the percentage differences of k_{app}, $T_{1/2}$ and $\eta(\%)$ values on the condition: maximum pH value of 9.2, MB concentration of ~12 mg L^{-1}, light intensity of ~220 μW cm^{-2}, Aeroxide® P25 concentration of 4 g L^{-1} and agitation speeds of 600 rpm, compared with the condition: maximum UVA light intensity of 412 μW cm^{-2}, MB concentration of ~12 mg L^{-1}, Aeroxide® P25 concentration of 4 g L^{-1}, pH 4.9 (natural pH) and agitation speed of 1000 rpm, are 11.11%, 11.33% and 0.98%, respectively, on the photocatalytic degradation of MB using Aeroxide® P25 as a photocatalyst from decreasing pH value and increasing amount of UVA light intensity as ~2 times. The percentage differences of k_{app}, $T_{1/2}$ and $\eta(\%)$ values on the condition: maximum pH value of 9.2, MB concentration of ~12 mg L^{-1}, Aeroxide® P25 concentration of 4 g L^{-1}, light intensity of ~220 μW cm^{-2} and agitation speed of 600 rpm, compared with the condition: maximum agitation speed of

2500 rpm MB concentration of ~12 mg L^{-1}, Aeroxide® P25 concentration of 4 g L^{-1}, pH 4.9 (natural pH) and light intensity of ~220 μW cm^{-2}, are 0.00%, 0.14% and 1.36%, respectively, on the photocatalytic degradation of MB using Aeroxide® P25 as a photocatalyst from decreasing pH and increasing agitation speed values as ~2 and ~4 times, respectively. Those indicate that UVA light intensity gives is more significant to MB photocatalytic degradation than pH and agitation speed, and pH gives same significance on MB photocatalytic degradation as agitation speed. The percentage differences of k_{app}, $T_{1/2}$ and $\eta(\%)$ values on the condition: optimal Aeroxide® P25 concentration of 4–5 g L^{-1}, MB concentration of ~12 mg L^{-1}, light intensity of ~220 μW cm^{-2}, pH 4.9 (natural pH) and agitation speed of 1000 rpm, compared with the condition: maximum agitation speed of 2500 rpm MB concentration of ~12 mg L^{-1}, Aeroxide® P25 concentration of 4 g L^{-1}, pH 4.9 (natural pH) and light intensity of ~220 μW cm^{-2}, are 20.83%, 27.37% and 5.55%, respectively, on the photocatalytic degradation of MB using Aeroxide® P25 as a photocatalyst from increasing agitation speed as ~2 times, respectively.

The influential parameters were arranged in order of MB degradation performance in the suspension photoreactor using Aeroxide® P25/TiO_2 as a photocatalyst as follows: UVA light intensity > agitation speed $\cong$ pH > concentration of Aeroxide® P25. Moreover, the optimal condition for operating MB photocatalytic degradation using Aeroxide® P25 as a photocatalyst in our system was found as the result: MB concentration of ~12 mg L^{-1}, Aeroxide® P25 concentration of 4-5 g L^{-1}, pH 9.2, light intensity of 412 μW cm^{-2} and agitation speed of 2500 rpm. This is similar to the previous research of H. Moradi et al. and M.H. Rasoulifard et al. which revealed that UV intensity was the most effective parameter on photocatalytic decolorization on reactive yellow 84 using ZnO as a photocatalyst [36] and on Basic Red 46 using Zn_2SnO_4 as a photocatalyst [37]. However, there are some previous reports in different systems on photocatalytic degradations of toxic organic molecules. For examples, N. Setarehshenas et al. [38] reported that the parameter showing the highest efficiency percentage (~60.65%) on basic red 46 (BR46) degradation using ZrO_2-C as a photocatalyst was pH of solution. A. Giraldo et al. [39] reported that pH was especially important parameter on degradation of the antibiotic oxolinic acid using TiO_2 (Degussa P25) as a photocatalyst through photocatalysis process. S.A. Hosseini et al. [40] showed that pH was the most important parameter affecting degradation of methylene blue using ZnO as a photocatalyst. Likewise, J.-H. Kim et al. [41] revealed that pH value affects dispersion stability relating to diffusion/ convection mass transfer of photocatalyst nanoparticles in medium which is a key parameter for improving MB photocatalytic degradation efficiency. Moreover, B. Lopez- Alvarez et al. [42] reported that the most important variable on photocatalytic treatment of carbofuran using TiO_2 as a photocatalyst is concentration of the photocatalyst.

Table 2. The trends of the operational parameters for MB photocatalytic degradation in the suspension photoreactor.

Operational Parameter	Equation	R^2	Function	Equation No.
Aeroxide® P25 Concentration	$y = \exp(-3.84704 + 0.25828x - 0.02814x^2)$	0.95847	Exp3p2 exponential	(3.4)
pH at 0 rpm	$y = \exp(-5.53811 + 0.11506x + 0.01424x^2)$	N/A	Exp3p2 exponential	(3.5)
pH at 600 rpm	$y = \exp(-2.9332 - 0.25826x + 0.02659x^2)$	N/A	Exp3p2 exponential	(3.6)
Agitation speed	$y = 0.00357x^{0.32382}$	0.72972	Allometric power	(3.7)
UVA light intensity	$y = (0.03168 - 6.22581 \times 10^{-5}x) / (1 - 0.00216x)$	0.64736	Rational	(3.8)

Table 3. The k_{app}, $T_{1/2}$ and $\eta\%$ values of the highest MB photocatalytic degradation in each of the operational parameters.

Parameter	Amount	Condition	k_{app} (min^{-1})	$T_{1/2}$ (min) (this research)	$\eta(\%)$ at 90 min (this research)
Concentration of Aeroxide® P25	4–5 g L^{-1}	MB concentration of ~12 mg L^{-1}, light intensity of ~ 220 µW cm^{-2}, pH 4.9 (natural pH) and agitation speed of 1000 rpm	0.038	18.24	94.18
pH at 0 rpm	9.2	MB concentration of ~12 mg L^{-1}, Aeroxide® P25 concentration of 4 g L^{-1}, light intensity of ~220 µW cm^{-2} and agitation speed of 0 rpm	0.040	17.34	95.75
pH at 600 rpm	9.2	MB concentration of ~12 mg L^{-1}, Aeroxide® P25 concentration of 4 g L^{-1}, light intensity of ~220 µW cm^{-2} and agitation speed of 600 rpm	0.048	14.34	98.36
Agitation speed	2500 rpm	MB concentration of ~12 mg L^{-1}, Aeroxide® P25 concentration of 4 g L^{-1}, pH 4.9 (natural pH) and light intensity of ~220 µW cm^{-2}	0.048	14.32	99.72
UVA light intensity	412 µW cm^{-2}	MB concentration of ~12 mg L^{-1}, Aeroxide® P25 concentration of 4 g L^{-1}, pH 4.9 (natural pH) and agitation speed of ~1000 rpm	0.054	12.88	99.33

4. Conclusion

Experimental investigation of MB degradation using Aeroxide® P25 as a photocatalyst in the suspension photoreactor was made by separately analyzing each operational parameter affecting apparent MB degradation rate constant (k_{app}). The trends of the k_{app} value as a function of Aeroxide® P25 concentration and pH value are similar as an Exp3p2 exponential function. The trend of the k_{app} value as a function of agitation speed corresponds to an allometric function. The trend of the k_{app} value as a function of light intensity corresponds to a rational function. The pH parameter affects the stability of Aeroxide® P25 particles in water. In neutral pH, the particles agglomerated and quickly fell in water; in contrast, the particles dispersed and slowly fell in water in strong basic and acidic conditions. The operational parameters were ranked in order of influence on MB degradation performance from using Aeroxide® P25 as a photocatalyst in the

suspension photoreactor, greatest first, as follows: UVA light intensity, agitation speed/pH and concentration of Aeroxide® P25. For guidance to future work related to MB photocatalytic degradation, the operational parameters of pH and light region should be adjusted corresponding with the photocatalyst type. On the investment evaluation, it is possible that the quantities of the operational parameters would be converted to prices before the investment.

Acknowledgments

References
[1] Vutskits L, Briner A, Klauser P, Gascon E, Dayer AG, Kiss JZ, et al. Adverse effects of methylene blue on the central nervous system. Anesthesiology. 2008; 108:684-92.

[2] Gillman PK. Methylene blue implicated in potentially fatal serotonin toxicity. Anaesthesia. 2006;61:1013-4.

[3] Ginimuge PR, Jyothi SD. Methylene blue: revisited. J Anaesthesiol Clin Pharmacol. 2010;26:517-20.

[4] Majithia A, Stearns MP. Methylene blue toxicity following infusion to localize parathyroid adenoma. J Laryngol Otol. 2006;120:138-40.

[5] Wang X, Liu M, Yang Z. Coupled model based on radiation transfer and reaction kinetics of gas-liquid-solid photocatalytic mini-fluidized bed. Chem Eng Res Des. 2018;134:172-85.

[6] Rahman QI, Ahmad M, Misra SK, Lohani M. Efficient degradation of methylene blue dye over highly reactive Cu doped strontium titanate ($SrTiO_3$) nanoparticles photocatalyst under visible light. J Nanosci Nanotechnol. 2012;12:7181-6.

[7] Zhou C, Zhang W, Wang H, Li H, Zhou J, Wang S, et al. Preparation of Fe_3O_4-embedded graphene oxide for removal of methylene blue. Arab J Sci Eng. 2014;39:6679-85.

[8] Wang J, Nonami T. Photocatalytic activity for methylene blue decomposition of $NaInO_2$ with a layered structure. J Mater Sci. 2004;39:6367-70.

[9] Ahmad M, Iqbal Z, Hong Z, Yang J, Zhang Y, Khalid NR, et al. Enhanced sunlight photocatalytic performance of hafnium doped ZnO nanoparticles for methylene blue degradation. Integr Ferroelectr. 2013;145:108-14.

[10] Thilagavathi P, Manikandan A, Sujatha S, Jaganathan SK, Arul Antony S. Sol-gel synthesis and characterization studies of $NiMoO_4$ nanostructures for photocatalytic degradation of methylene blue dye. Nanosci Nanotechnol Lett. 2016;8:438-43.

[11] Pouretedal HR, Sabzevari S. Photodegradation study of congo red, methyl orange, methyl red and methylene blue under simulated solar irradiation catalyzed by ZnS/CdS nanocomposite. Desalin Water Treat. 2011;28:247-54.

[12] Kumar PS, Karuthapandian S, Umadevi M, Elangovan A, Muthuraj V. Light induced synthesis of Sr/CdSe nanocomposite for the highly synergistic photodegradation of methylene blue dye solution. Mater Focus. 2016;5:128-36.

[13] Yu J, Yu H, Cheng B, Zhou M, Zhao X. Enhanced photocatalytic activity of TiO_2 powder (P25) by hydrothermal

treatment. J Mol Catal A-Chem. 2006;253:112-8.

[14] Ohno T, Sarukawa K, Tokieda K, Matsumura M. Morphology of a TiO$_2$ photocatalyst (Degussa, P-25) consisting of anatase and rutile crystalline phases. J Catal. 2001;203:82-6.

[15] Hurum DC, Agrios AG, Gray KA, Rajh T, Thurnauer MC. Explaining the enhanced photocatalytic activity of Degussa P25 mixed-phase TiO$_2$ using EPR. J Phys Chem B. 2003;107:4545-9.

[16] Jiang X, Manawan M, Feng T, Qian R, Zhao T, Zhou G, et al. Anatase and rutile in evonik aeroxide P25: Heterojunctioned or individual nanoparticles? Catal Today. 2018;300:12-7.

[17] Houas A, Lachheb H, Ksibi M, Elaloui E, Guillard C, Herrmann J-M. Photocatalytic degradation pathway of methylene blue in water. Appl Catal B-Environ. 2001;31:145-57.

[18] Singh N, Rana MS, Gupta RK. Modelling studies for photocatalytic degradation of organic dyes using TiO$_2$ nanofibers. Environ Sci Pollut Res. 2018;25:20466-72.

[19] Allahveran S, Mehrizad A. Polyaniline/ZnS nanocomposite as a novel photocatalyst for removal of Rhodamine 6G from aqueous media: Optimization of influential parameters by response surface methodology and kinetic modeling. J Mol Liq. 2017;225:339-46.

[20] Ebrahimi M, Yousefzadeh S, Samadi M, Dong C, Zhang J, Moshfegh AZ. Facile preparation of branched hierarchical ZnO nanowire arrays with enhanced photocatalytic activity: A photodegradation kinetic model. Appl Surf Sci. 2018;435:108-16.

[21] Rajeshwar K, Osugi ME, Chanmanee W, Chenthamarakshan CR, Zanoni MVB, Kajitvichyanukul P, et al. Heterogeneous photocatalytic treatment of organic dyes in air and aqueous media. J Photoch Photobio C. 2008;9:171-92.

[22] Fernández-Ibáñez P, de las Nieves FJ, Malato S. Titanium dioxide/electrolyte solution interface: electron transfer phenomena. J Colloid Interf Sci. 2000;227:510-6.

[23] Rasoulifard MH, Seyed Dorraji MS, Amani-Ghadim AR, Keshavarzbabaeinezhad N. Visible-light photocatalytic activity of chitosan/ polyaniline/CdS nanocomposite: Kinetic studies and artificial neural network modeling. Appl Catal A-Gen. 2016;514:60-70.

[24] Camarillo R, Rincón J. Photocatalytic discoloration of dyes: Relation between effect of operating parameters and dye structure. Chem Eng Technol. 2011;34:1675-84.

[25] Michalow KA, Flak D, Heel A, Parlinska-Wojtan M, Rekas M, Graule T. Effect of Nb doping on structural, optical and photocatalytic properties of flame-made TiO$_2$ nanopowder. Environ Sci Pollut Res. 2012;19:3696-708.

[26] Wu C-H, Chang H-W, Chern J-M. Basic dye decomposition kinetics in a photocatalytic slurry reactor. J Hazard Mater. 2006;137:336-43.

[27] Daneshvar N, Salari D, Khataee AR. Photocatalytic degradation of azo dye acid red 14 in water: investigation of the effect of operational parameters. J Photoch Photobio A. 2003;157:111-6.

[28] Peter A, Mihaly-Cozmuta A, Nicula C, Mihaly-Cozmuta L, Jastrzębska A, Olszyna A, et al. UV light-assisted degradation of methyl orange, methylene blue, phenol, salicylic acid, and rhodamine B: photolysis versus

photocatalyis. Water Air Soil Poll. 2017;228:41.

[29] Davis ME, Davis RJ. Fundamentals of chemical reaction engineering: Courier Corporation; 2012.

[30] Wang T, Li Y, Pan JH, Zhang YL, Wu LG, Dong CY, et al. Alcohol solvothermal reduction for commercial P25 to harvest weak visible light and fabrication of the resulting floating photocatalytic spheres. Sci Rep. 2019;9:1-11.

[31] Guo H-X, Lin K-L, Zheng Z-S, Xiao F-B, Li S-X. Sulfanilic acid-modified P25 TiO_2 nanoparticles with improved photocatalytic degradation on Congo red under visible light. Dyes Pigments. 2012;92:1278-84.

[32] Liang BY, Han DH, Zhang WX, Zhang YL, Zhang RJ, Zhang TC, et al. Surface-decorated SnO nanoflowers with P25 for enhanced visible light photocatalytic degradation of MO. J Aust Ceram Soc. 2019;55:825-9.

[33] Egerton TA, Mattinson JA. The influence of platinum on UV and 'visible' photocatalysis by rutile and Degussa P25. J Photoch Photobio A. 2008;194:283-9.

[34] Jin Z, Duan W, Duan WB, Liu B, Chen XD, Yang FH, et al. Indium doped and carbon modified P25 nanocomposites with high visible-light sensitivity for the photocatalytic degradation of organic dyes. Appl Catal A-Gen. 2016;517:129-40.

[35] Yang Y, Zhang T, Le L, Ruan X, Fang P, Pan C, et al. Quick and facile preparation of visible light-driven TiO_2 photocatalyst with high absorption and photocatalytic activity. Sci Rep. 2014;4:7045.

[36] Moradi H, Sharifnia S, Rahimpour F. Photocatalytic decolorization of reactive yellow 84 from aqueous solutions using ZnO nanoparticles supported on mineral LECA. Mater Chem Phys. 2015;158:38-44.

[37] Rasoulifard M, Dorraji MS, Taherkhani S. Photocatalytic activity of zinc stannate: preparation and modeling. J Taiwan Inst Chem Eng. 2016;58:324-32.

[38] Setarehshenas N, Hosseini SH, Ahmadi G. Optimization and kinetic model development for photocatalytic dye degradation. Arab J Sci Eng. 2018;43:5785-97.

[39] Giraldo AL, Penuela GA, Torres-Palma RA, Pino NJ, Palominos RA, Mansilla HD. Degradation of the antibiotic oxolinic acid by photocatalysis with TiO_2 in suspension. Water Res. 2010;44:5158-67.

[40] Hosseini SA, Babaei S. Graphene oxide/zinc oxide (GO/ZnO) nanocomposite as a superior photocatalyst for degradation of methylene blue (MB)-process modeling by response surface methodology (RSM). J Braz Chem Soc. 2017;28:299-307.

[41] Kim J-H, Nishimura F, Yonezawa S, Takashima M. Enhanced dispersion stability and photocatalytic activity of TiO_2 particles fluorinated by fluorine gas. J Fluorine Chem. 2012;144:165-70.

[42] Lopez-Alvarez B, Torres-Palma RA, Peñuela G. Solar photocatalitycal treatment of carbofuran at lab and pilot scale: effect of classical parameters, evaluation of the toxicity and analysis of organic by-products. J Hazard Mater. 2011;191:196-203.